

Received February 5, 2020, accepted February 21, 2020, date of publication February 27, 2020, date of current version March 11, 2020.

Digital Object Identifier 10.1109/ACCESS.2020.2976902

Improved Mapping of Soil Heavy Metals Using a Vis-NIR Spectroscopy Index in an Agricultural Area of Eastern China

JIANFEI CAO¹, CHUNFANG LI¹, QUANYUAN WU¹, AND JIANMIN QIAO¹

College of Geography and Environment, Shandong Normal University, Jinan 250014, China

Corresponding authors: Quanyuan Wu (wqy6420582@163.com) and Jianmin Qiao (qjmwilson@163.com)

This work was supported in part by the National Natural Science Foundation of China under Grant 41371395, in part by the Natural Science Foundation of Shandong Province under Grant ZR2017BD011, in part by the China Postdoctoral Science Foundation under Grant 2017M622256, and in part by the Key Technology Research and Development Program of Shandong under Grant 2017CXGC304 and Grant 2019GSF109034.

ABSTRACT Visible and near-infrared reflectance (Vis-NIR) spectroscopy can provide low-cost and high-density data for mapping various soil properties. However, a weak correlation between the spectra and measurements of soil heavy metals makes spectroscopy difficult to use in predicting incipient risk areas. In this study, we introduce a new spectral index (SI) based on Vis-NIR spectra and use it as a covariate in ordinary cokriging (OCK) to improve the mapping of soil heavy metals. The SI was defined from the highest covariance between spectra and heavy metal content in the partial least squares regression (PLSR) model. The proposed mapping approach was compared with an ordinary kriging (OK) predictor that uses only soil heavy metal data and an OCK predictor that uses soil organic matter (SOM) and Fe as covariates. To this end, a total of 100 topsoil (0–20 cm) samples were collected in an agricultural area near Longkou City, and the contents of As, Pb and Zn in the soil were determined. The results showed that OCK with the SI provided better results in terms of unbiasedness and accuracy compared to other comparative methods. Additionally, we explored the SI through simple strategies based on spectral analysis and correlation statistics and found that the SI synthesized most of the soil properties affected by heavy metals and was not limited to Fe and SOM. In summary, the SI method is cost-effective for improving soil heavy metal mapping and can be applied to other areas.

INDEX TERMS Soil heavy metals, digital soil mapping, Vis-NIR spectroscopy, geostatistics.

I. INTRODUCTION

Heavy metals are well known for their toxicity and persistence and their ability to directly affect agricultural ecology and food safety in cultivated soils [1]–[3]. The accumulation of heavy metals threatens human health because metals can enter the body through the food chain [4]. Generally, excessive heavy metals in farmlands mainly originate from anthropogenic activities, such as industrial activities, sewage irrigation and pesticide and fertilizer overuse [5]. The high density of human activities leads to a sharp increase in soil heavy metals at the local scale, which is directly manifested by the complex spatial variability in soil heavy metals. Therefore, obtaining efficient and accurate spatial variation information about soil heavy metals has become increasingly

important because such information is crucial to soil contamination remediation [6], [7].

Geostatistical methods with variography and spatial interpolation techniques have been widely used to predict the spatial distribution of soil heavy metals by providing unbiased estimates at unsampled sites [8], [9]. The spatial distribution of heavy metals in soils usually presents complex spatial variations due to the combination of various surface environmental factors and sources. Numerous studies have shown that the accuracy of spatial estimation is limited by univariate geostatistical techniques (e.g., inverse distance weighting, spline smoothing and ordinary kriging), which discern the total variation in one variable [8], [10]–[12]. Ordinary cokriging (OCK), which is based on the theory of collaborative regionalization variables, seems to be particularly attractive for interpreting complex spatial variations. OCK, using the correlation between multiple regionalization variables, has

The associate editor coordinating the review of this manuscript and approving it for publication was Qiangqiang Yuan¹.

been applied to soil science, environmental science, ecology and geochemistry [13]–[16].

Many environmental factors, including climate, topographic, vegetative and geologic conditions, have been applied as auxiliary variables in OCK to estimate soil properties [13], [14]. Environmental variables also play an important role in soil heavy metal prediction because they are easily measurable and indirectly affect the distribution of heavy metals [17], [18]. However, these geographical environments often exhibit high spatial similarity and do not reflect the complex spatial variation in soil heavy metals at small regional scales. Heavy metals inhibit the activities of biological plants and soil microorganisms [1]. In surface soils, heavy metals bind to organic matter and accelerate degradation; in addition, oxide metals and clay also decrease based on complex chemical reactions with soil [19]–[21]. Therefore, the physical and chemical properties of surface soils have a relationship with soil heavy metals. In particular, soil organic matter (SOM), Fe oxides, and clay provide effective auxiliary information and have been used to improve the prediction accuracy of heavy metals in soil [22]. However, the acquisition of physical and chemical properties in soils is time consuming and expensive and is unsuitable for mapping wide variability at the landscape scale.

In view of the inefficiency and low performance of environmental and soil property variables, we tried to find a substitute indicator. Hyperspectral remote sensing data have significant associations with soil properties but only in a cleared area of bare soil without vegetation [23]–[25]. Laboratory hyperspectral data, in which the region of the spectrum is in the visible (350–780 nm) and near-infrared (780–2500 nm) regions of the spectrum, provide high-spectral-resolution data that can capture the minor variability in soil properties. This efficient spectral information has also been directly used to evaluate heavy metals in soil through inversion models (e.g., partial least squares, artificial neural networks, and support vector machines [26]–[28]) but is mostly used in mining or industrial areas with high soil heavy metal contamination. Heavy metals in soil at low levels are deemed spectrally featureless, and most of them are difficult to directly detect with visible and near-infrared reflectance (Vis-NIR) reflectance spectroscopy [22]. In recent studies, the weak correlation between the spectra and measurements of soil properties was extracted as auxiliary information and integrated into a geostatistical analysis to make mapping easier and more accurate [29]–[31]. Although a few studies have applied Vis-NIR spectroscopy to assist the digital mapping of soil heavy metals, only sensitive wavelengths have been considered [32], [50]. Comprehensive Vis-NIR spectral information and multivariate geostatistics are expected to be efficient tools for predicting soil heavy metals.

Longkou is a typical industrial and mining area in coastal eastern China. Suburban agriculture provides most of the food and vegetables for Longkou City. However, long-term sewage irrigation and surrounding complex heavy metal emission sources have led to heavy metal accumulation in

agricultural soils [33]. In this study, we took the suburban agricultural area of Longkou as a typical experimental area. A spectral index (SI) based on laboratory Vis-NIR spectroscopy was integrated into multivariate geostatistics to improve the mapping of soil heavy metals. The main objectives were to 1) develop a SI based on Vis-NIR spectroscopy that synthesizes the most informative spectral variations, 2) use the SI as an auxiliary variable to better predict soil heavy metals in a geostatistical framework, and 3) propose a strategy for exploring the spectral index when applied to other areas.

II. MATERIALS AND METHODS

A. STUDY AREA

The study area is located in the northern plain of Longkou City in eastern China. This area has a temperate monsoon climate with an average annual temperature of 12 °C. The average annual rainfall in Longkou City is 586.3 mm, and 70% of the rain falls between May and September. The per capita water resources amount is 370 m³, which accounts for 14.8% of the national per capita amount of water in China. The average amount of groundwater in the area is 7545 m³/hm², which indicates a severe shortage of water in the region [34]. Industrial wastewater and domestic sewage have become the main supplementary water sources in Longkou. The area characterized by mineral resource exploitation, including coal, gold mine and lead zinc mining, and the abundant natural resources have promoted the development of preliminary industrial enterprises, such as iron-making plants, paper mills and electroplating factories. With the rapid development of industrial and mining enterprises in Longkou, the irrigated area was converted to a sewage irrigation area in 1984. Industrial and domestic raw wastewater and treated wastewater are discharged into the Huangshui River and the Yongwen River to irrigate farmland [33].

B. SAMPLE COLLECTION AND CHEMICAL ANALYSIS

A total of 100 surface soil samples (0–20 cm) were collected from the study area, as shown in Fig. 1. Grid sampling was performed, in which sample sites were selected according to a sampling density of less than 2 km. Each soil sample consisted of a mixture of five subsamples collected from five points in an area of approximately 30 m². All subsamples were collected at a depth of 0–20 cm using a stainless-steel shovel. One kilogram of the soil samples was transported to a laboratory. After natural air drying and debris removal, the soil samples were sieved to 0.84 mm. Each soil sample was split into two portions as follows: one part for spectral measurements and the other part for soil property analysis.

In the laboratory, the soil samples were ground to a fine powder with a particle size of less than 0.149 mm. HSO₄-HNO₃-HF was used to digest the soil for analyzing the As, Pb and Zn contents, which were then measured by inductively coupled plasma-atomic emission spectrometry [35]. Low-power X-ray fluorescence spectrometry was used to

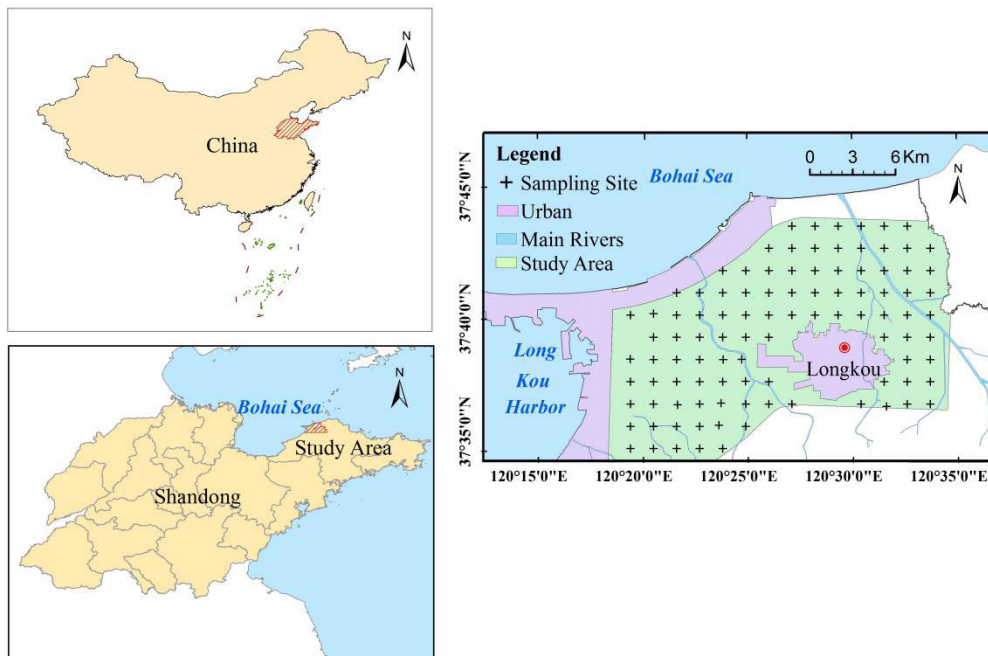


FIGURE 1. Study area and locations of the sampling sites.

determine the total Fe content [36]. The SOM content was determined through wet oxidation at 180 °C with a mixture of potassium dichromate and sulfuric acid [37]. The recovery rate and standard reference material were examined under strict monitoring, and the chemical analysis process followed the standard for the geochemical evaluation of land quality (DZ/T0295—2016) in China.

C. SPECTRAL MEASUREMENTS AND PRETREATMENTS

The soil was sieved and then placed into round aluminum boxes, which were then placed in a dark room. Soil spectra were measured using an ASD FieldSpec HandHeld 3 portable spectroradiometer (Analytical Spectra Devices, Inc., USA), which covers a wavelength range of 350-2500 nm. The detector is a low-noise, 512 pixel photodiode array with a spectral resolution of 3 nm (350-1000 nm) and 10 nm (1000-2500 nm) and sampling intervals of 1.4 nm (350-1000 nm) and 2 nm (1000-2500). We preheated the spectrometer for 20-30 minutes and calibrated it with a white-board before spectrum measurement. The stable light source was a 50 W halogen lamp. All of the measuring instruments were pointed vertically downward and maintained within at least $\pm 10^\circ$ of the normal line of the horizontal plane and approximately 30 cm away from the soil sample. To eliminate measurement instability, 10 spectral curves were collected for each soil sample [25].

Savitzky-Golay (SG) filtering was used to smooth the curve to eliminate the “burr” noise on the spectral curve, as shown in Fig. 2. The following SG parameters were selected: 0 order and 9 frame-len. These parameters obtained the best results based on a trial and error experiment, as shown

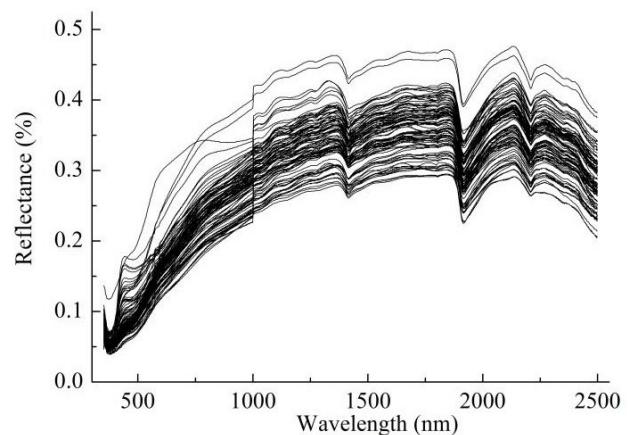


FIGURE 2. SG spectra of the soil samples ($n = 100$).

in Table 7. The reflectance data were transformed into first and second derivatives to reduce multicollinearity, as shown in Fig. 7(a) and Fig. 7(b). Baseline drift and multiple scattering effects were eliminated from the laboratory spectra through standard normal variate (SNV) correction and multiplicative scatter correction (MSC), as shown in Fig. 7(c) and Fig. 7(d).

D. Vis-NIR SPECTRAL INDEX DEFINITION

Each laboratory spectral set had thousands of spectral variables that needed to be compressed into an independent variable for spatial prediction. Partial least squares regression (PLSR), which can eliminate possible collinearity, has been widely used to estimate chemical content from spectral

information [27], [28] and [38]. In addition, PLSR can be used not only for regression prediction but also for the extraction of one or a few potential factor variables of the spectra that synthesize most of the covariance in the dependent and independent variables [29]. For this reason, those factor variables were defined as the SI using the partial least squares method for characterizing soil heavy metal variation. The leave-one-out cross-validation method was used to determine the optimal factor number that retained the minimum value of the root mean square error (RMSE) in the model [39]. The variable importance in the projection (VIP) was computed to evaluate the most relevant predictors for response variable prediction [40]. If the VIP value is larger than 1 and the b-coefficient value is larger than the standard deviation, the corresponding wavelength is considered important. PLSR was performed using SAS/STAT version 9.3 (SAS Inc. USA).

E. GEOSTATISTICAL METHODS

1) ORDINARY KRIGING AND ORDINARY COKRIGING

The spatial variability in heavy metals was described using both univariate (OK) and multivariate (OCK) geostatistics. Variograms are the basis of kriging interpolation and are used to represent the spatial variation structure of regional variables based on regionalized variable theory and inherent assumptions. For a data set for variable $Z(x_i)$ at n locations, the variogram $\gamma(h)$ is expressed as (1).

$$\gamma(h) = \frac{1}{2N(h)} \sum_{i=1}^{N(h)} [Z(x_i) - Z(x_i+h)]^2 \quad (1)$$

where h is the vector between the two sample points; $Z(x_i)$ and $Z(x_i+h)$ are the observed values of $Z(x)$ in space x and $x+h$, respectively [$i = 1, 2 \dots N(h)$]; and $N(h)$ is the number of sample pairs.

Given multiple data sets for the primary variable $Z_i(x_i)$ and the auxiliary variable $Z_j(x_j)$, cross-variograms are calculated by (2).

$$\gamma(h) = \frac{1}{2N(h)} \sum_{i=1}^{N(h)} [Z_i(x_i) - Z(x_i+h)] * [Z_j(x_j) - Z(x_j+h)] \quad (2)$$

If the variogram indicates that the variable is spatially dependent, then the unbiased optimal estimation of regionalized variables in a limited region is carried out for the OK prediction based on an analysis of the variogram structure. The OK can be expressed as (3).

$$\tilde{y}(x_0) = \sum_{i=1}^n \lambda_i Z(x_i) \quad (3)$$

where \tilde{y} is the predicted value at the x_0 location, $Z(x_i)$ is the corresponding measurement, λ_i is the weight per measurement point, and $i = 1, 2 \dots N$.

The cokriging interpolation method is an unbiased optimal estimation based on a cross-variogram and is expressed

by (4).

$$\tilde{y}(x_0) = \sum_{i=1}^m \lambda_{1i} Z_1(x_i) + \sum_{i=1}^m \lambda_{2i} Z_2(x_j) \quad (4)$$

where $Z_1(x_i)$ is the measurement of the primary variable x_i and $Z_2(x_j)$ is the measurement of the auxiliary variable x_j . λ_{1i} and λ_{2i} are the weights of Z_1 and Z_2 , respectively. $i = 1, 2 \dots M$, and $j = 1, 2 \dots Q$.

In this study, soil heavy metals were spatially predicted using OK and OCK with the covariates SI, SOM and Fe in the agricultural study area. To investigate the SI for the spatial evaluation of soil heavy metals, the SI was first used as the primary variable for OK to compare the spatial patterns of soil heavy metals. Second, the SI was used as an auxiliary variable for OCK to determine whether the SI could be considered an effective surrogate for the soil properties expected to improve the accuracies of soil heavy metal maps.

Kriging interpolation requires that the variable be close to a normal distribution for higher efficiency and lower system error. Therefore, statistical analyses, including data transformations (log and Gaussian) and the Kolmogorov-Smirnov (K-S) test, with P values less than 0.05, were performed in MATLAB (2015) (MathWorks Inc., USA). The variograms and parameters were executed in GS+ 7.0 (Gamma Design Software LLC, USA). OK and OCK were implemented with the ArcGIS geostatistics tool (ESRI Inc., USA).

2) CROSS-VALIDATION

Cross-validation statistics were used to evaluate and compare the prediction results of OK and OCK with the different variables. Performance indicators, including the mean standard error (MSE), RMSE and root mean square standardized error (RMSDE), are expressed by (5), (6) and (7), respectively.

$$MSE = \frac{1}{n} \sum_{i=1}^n \frac{e_i}{\sigma_i} \quad (5)$$

$$RMSE = \left(\frac{1}{n} \sum_{i=1}^n e_i^2 \right)^{\frac{1}{2}} \quad (6)$$

$$RMSDE = \left(\frac{1}{n} \sum_{i=1}^n \frac{e_i^2}{\sigma_i^2} \right)^{\frac{1}{2}} \quad (7)$$

where $e_i = Y_i - \hat{Y}_i$ is the difference between the observed response value, Y_i , removed at the i th iteration and the predicted value, \hat{Y}_i obtained by fitting the model to the remaining $n-1$ points and σ_i is the mean squared prediction error of \hat{Y}_i .

The MSE was used to assess the unbiasedness of the predictor, and the optimal value of the MSE should be approximately zero [29], [42]. The RMSE was used to check the goodness of fit of the prediction, and models with smaller RMSE values are preferred because a low RMSE means that the fitted values are close to the observed values [43]. The RMSDE was used to assess the accuracy of the root

TABLE 1. Statistical description of the soil properties (n = 100).

	Unit	Min	Max	Mean	S.D. ^a	CV(%) ^b	Skewness	Background ^c	Level II of EQSS ^d
As	mg kg ⁻¹	4.55	12.63	8.06	3.15	39.03	2.78	6.30	30
Pb	mg kg ⁻¹	11.39	195.7	36.48	24.68	67.65	5.16	25.40	300
Zn	mg kg ⁻¹	29.44	187.7	62.59	25.33	40.47	3.46	56.10	250
SOM	g kg ⁻¹	0.34	3.07	1.53	0.51	33.33	1.41	-	-
Fe	g kg ⁻¹	0.85	4.66	2.42	0.62	25.62	0.80	-	-
pH	-	7	7.89	7.43	0.18	2.42	-0.01	-	-

^a S.D.: Standard deviation.

^b CV%: coefficient of variation in %.

^c Background value: Soil background values in Shandong Province (China National Environmental Monitoring Center, 1990).

^d Level II of EQSS: Level II of the Environmental Quality Standard for Soils (EQSS) of China (State Environmental Protection Administration of China, 1997).

TABLE 2. The covariances in the SIs of As, Pb, and Zn under different spectral pretreatments (%).

	Savitzky-Golay		First derivative		Second derivative		Standard normal variate transformation		Multiplicative scatter correction	
	predictor	response	predictor	response	predictor	response	predictor	response	predictor	response
As	72	8	33	20	33	20	70	4	72	4
Pb	89	10	45	13	45	13	69	3	69	4
Zn	89	8	53	6	63	6	72	3	73	2

mean square standardized prediction error and should be approximately 1.

F. Vis-NIR SI EVALUATION

We attempted to evaluate the SI by analyzing the relationship between soil heavy metals and active soil properties (e.g., SOM and Fe). A strategy that involves Spearman's correlation and partial correlation analyses was proposed. Spearman correlation coefficients were used to evaluate the relationship between paired variables [36]. Partial correlation analysis was used to test conditional independence, i.e., whether the relationship between two variables is controlled by potential influencing factors [41]. Therefore, Spearman's correlation and partial correlation analyses could fully reveal the relationship between heavy metals and the auxiliary variables.

III. RESULTS

A. DESCRIPTIVE STATISTICS

Table 1 summarizes the descriptive statistics for As, Pb, Zn, SOM, Fe and pH. The mean soil pH value was 7.43, suggesting that the soils were neutral in the study area. The mean contents of SOM and Fe were 1.53 and 2.42 g kg⁻¹, respectively, corresponding to coefficients of variation (CVs) of 33.33% and 25.62%, respectively. The mean contents of As, Pb and Zn were 8.06, 36.48, and 62.59 g kg⁻¹, respectively. Overall, the average heavy metal contents in all samples were below level II of the Environmental Quality Standard for Soils (EQSS) of China [44] but exceeded the corresponding

background values [45] by 1.28, 1.44 and 1.12 times, respectively. These results indicated that As, Pb and Zn were slightly enriched in the study area. The CVs of As, Pb and Zn were 39.03%, 67.65% and 40.47%, respectively. The heavy metal contents coupled with the high CV values suggest that their primary source may be human activities. In addition, these heavy metals are strongly positively skewed in the descending order of Pb (5.16) > Zn(3.46) > As(2.78), indicating that the heavy metal content level presents spatial variation with few very high values, especially for Pb and Zn.

B. SPECTRAL INDICES OF SOIL HEAVY METALS

In this study, seven factors were determined by the leave-one-out cross-validation method. The first factor accounted for most of the variation in predictors and was the only retained factor used as a new variable – the SI – for investigating heavy metals in soils. The covariances in the SIs of As, Pb and Zn under different spectral pretreatments are shown in Table 2. The SIs obtained from the first- and second-derivative spectral data contain less variance in the predictor variables (spectral information), and the SIs obtained from the SNV and MSC data almost ignore the response variable data (heavy metal content). The SIs showed satisfactory results when the PLSR analysis was performed on the SG spectral data (Fig. 2), which explained more variation in the predictors (As (72%), Pb (89%) and Zn (89%).

The important wavelengths of SOM, Fe and the three heavy metals mostly overlapped with those of the

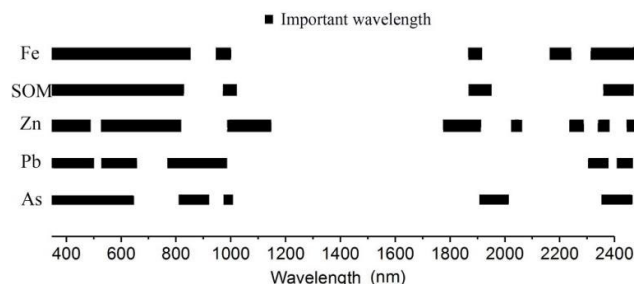


FIGURE 3. Plot of important wavelengths based on VIP using PLSR.

TABLE 3. Optimal variogram models of the log-transformed contents of As, Pb and Zn.

	Model	Nugget (C ₀)	Sill (C ₀ +C)	Proportion C ₀ /(C ₀ +C)	Range (A)/km	R ²
Lg As	Gaussian	0.018	0.026	0.69	11.8	0.72
Lg Pb	Gaussian	0.023	0.096	0.24	4.48	0.66
Lg Zn	Spherical	0.009	0.016	0.56	5.54	0.78

SG pretreatment method. In more detail, values higher than 1 were in the wavelength ranges of 350-1100 nm and 1900-2500 nm.

C. SPATIAL PREDICTION OF SOIL HEAVY METALS

The variograms were modeled, and the structural variabilities in heavy metals are shown in Table 3. The Gaussian theoretical models were the optimal variogram models for As and Pb, with R² values of 0.72 and 0.66, respectively. The spherical theoretical model was the optimal variogram model for Zn, with an R² value of 0.78. The spatial structures of As, Pb and Zn had values of 11.8, 4.48 and 5.54 km, respectively, and had C₀/(C₀ + C) values of 0.69, 0.24 and 0.56, respectively. The higher C₀/(C₀ + C) value and the larger effective variation range (Table 3) indicated that As and Zn had low levels of spatial dependence and association. The effective spatial autocorrelation scale of Pb was small, and the C₀/(C₀+C) value was less than 0.25, indicating that the spatial variation structure of Pb showed locally high spatial dependence and association. However, the high variance in descriptive statistics suggests that Pb had some extreme values.

The predicted maps of heavy metals were obtained using different interpolation methods, including OK and OCK with covariates (SI, SOM and Fe), as shown in Fig. 4, Fig. 5 and Fig. 6. As expected, under visual inspection, the kriged maps of heavy metals and cokriged maps with covariates showed similar spatial patterns. In contrast, the kriged maps of SIs (As, Pb and Zn) were quite different from the corresponding spatial pattern, indicating that SIs cannot be directly used to evaluate heavy metals in the studied agricultural area. Furthermore, the results of the cross-validation statistics (Table 4) showed that all of the ASE values were close to 0, the RMSE values were small, and the RMSDE values were close to 1, suggesting that the performances of these approaches satisfied the spatial prediction of heavy metals.

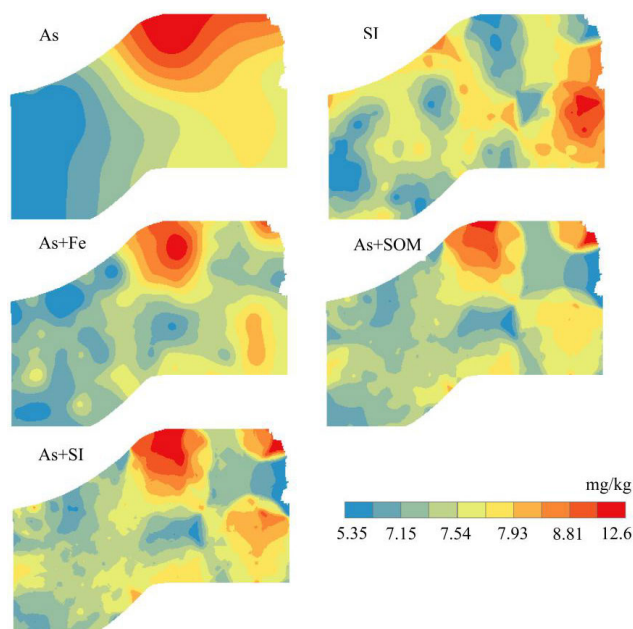


FIGURE 4. Predicted maps of As using OK and OCK with covariates Fe, SOM and SI.

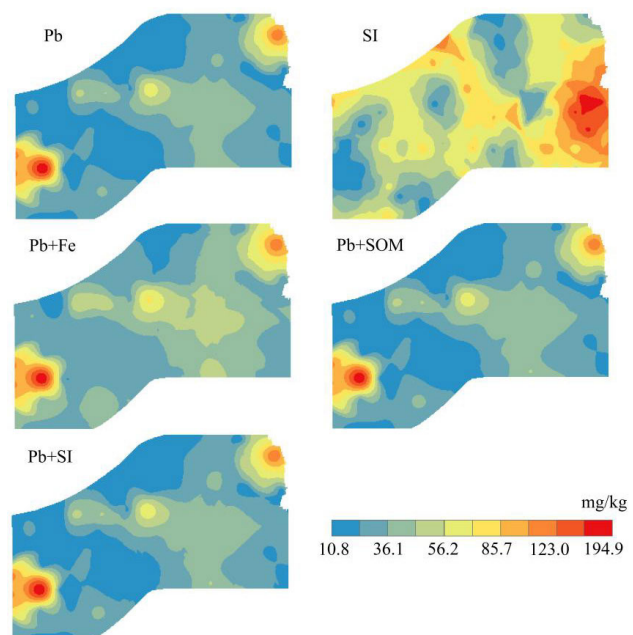


FIGURE 5. Predicted maps of Pb using OK and OCK with covariates Fe, SOM and SI.

In Fig. 4, the kriged map of As exhibited a gradual increase from west to east, and extreme values occurred in the northeast region. The cokriged maps of As with covariates of SOM, Fe, and SI exhibited more detail. Cross-validation of the predictions for As had ASE values ranging from -0.0421 to -0.0011, RMSE values ranging from 1.6127 to 1.8392, and RMSDE values ranging from 1.0264 to 1.1691 (Table 4). For both the unbiasedness (ASE) and accuracy (RMSE), the descending order of accuracy was OCK-SI>OCK-SOM>OCK-Fe>OK-As. For the

TABLE 4. Cross-validation test of the prediction of heavy metal contents using OK and OCK with Fe, SOM and SI as covariates.

	Method	ASE	RMSE	RMSDE
As	OK-As	-0.0014	1.8270	1.1691
	OCK-Fe	-0.0013	1.6794	1.0961
	OCK-SOM	-0.0421	1.8392	1.0553
	OCK-SI	-0.0011	1.6127	1.0264
Pb	OK-Pb	0.0040	27.8266	1.1476
	OCK-Fe	-0.0039	27.2786	1.1683
	OCK-SOM	0.0065	27.9936	1.1581
Zn	OCK-SI	0.0038	27.6210	1.1773
	OK-Zn	-0.0135	12.3129	1.0626
	OCK-Fe	-0.0182	12.0083	1.1453
	OCK-SOM	-0.0162	12.0143	1.0256
	OCK-SI	-0.0103	12.0023	1.0001

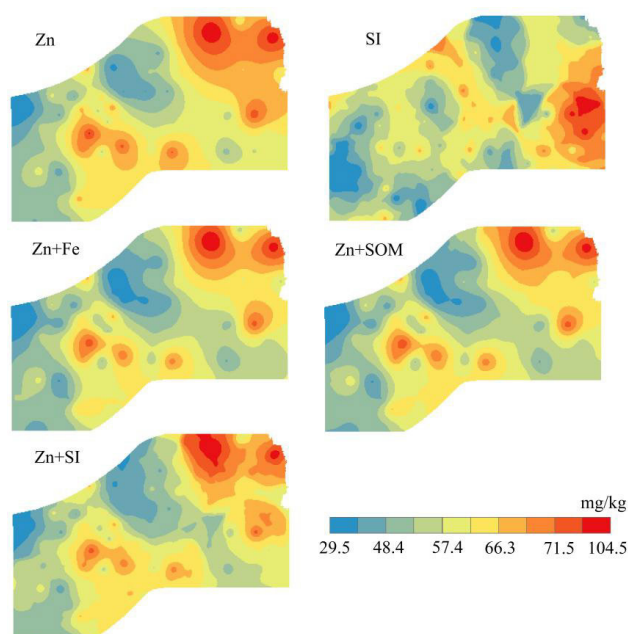
accuracy (RMSDE), OCK-SI and OCK-Fe performed better than OK-As. Therefore, the predicted map using Fe or SI as a covariate was more accurate than that using As or SOM as a covariate.

In Fig. 5, the kriged map of Pb has two high-value areas in the west and northeast and was quite consistent with the OCK results with different covariates. Cross-validation of the prediction of Pb had ASE values ranging from -0.0039 to 0.0065 , RMSE values ranging from 27.2786 to 27.9936 , and RMSDE values ranging from 1.1476 to 1.1683 (Table 4). For both the unbiasedness (ASE) and accuracy (RMSE), the descending order of accuracy was $\text{OCK-SI} > \text{OCK-Fe} > \text{OK-Pb} > \text{OCK-SOM}$. However, OK-Pb performed better than other predictions in terms of accuracy (RMSDE). These results indicated that the covariates of Fe, SOM and SI did not aid in the evaluation of Pb and even led to a slight decline in the prediction accuracy.

In Fig. 6, the high-value areas for Zn were in the central and northeast regions of the study area. Cross-validation of the prediction of Zn had ASE values ranging from -0.0103 to -0.0182 , RMSE values ranging from 12.0023 to 12.3129 , and RMSDE values ranging from 1.0001 to 1.1453 (Table 4). For both the unbiasedness (ASE) and accuracy (RMSE and RMSDE), the descending order of accuracy was $\text{OCK-SI} > \text{OCK-SOM} > \text{OCK-Fe} > \text{OK-Zn}$. Therefore, using Fe, SOM or SI as covariates could improve the prediction accuracy for Zn, especially when using the SI, which had the best performance.

D. DCORRELATION ANALYSIS AND PARTIAL CORRELATION ANALYSIS

The correlation coefficients (r) of the Spearman correlation and partial correlation with a significance level of 0.01 between the heavy metals and covariables (Fe, SOM and SI) are shown in Table 5. As and Zn had a significant correlation with these covariables, and the absolute values of the correlations ranged from 0.220 to 0.338 . Pb showed

**FIGURE 6.** Predicted maps of Zn using OK and OCK with covariates Fe, SOM and SI.

a low significant correlation with the SI but no significant correlation with Fe or SOM. When the Fe content was controlled, As, Pb and Zn were no longer significantly correlated with the SI, while the correlation with SOM was slightly reduced. Additionally, the correlations of Pb and Zn with the SI were not significant when the SOM contents were controlled. In addition, no significant correlations were found between all heavy metals and the corresponding SI when the SOM and Fe contents were controlled simultaneously. Overall, the results for the Spearman correlation and partial correlation indicated that SOM and Fe cannot be ignored in investigations of the relationships between heavy metals and the Vis-NIR SI.

TABLE 5. Spearman correlation coefficients (r) between the heavy metals and covariables and the partial correlation coefficients with controlled SOM and/or Fe ($n = 100$).

	Method	Category	SI	Fe	SOM
As	Spearman correlation coefficient		-0.312*	0.220*	0.281*
	Partial correlation coefficient	Fe controlled	-0.181		
		SOM controlled	-0.397*		
		Fe and SOM controlled	-0.175		
Pb	Spearman correlation coefficient		-0.242*	0.316	0.234
	Partial correlation coefficient	Fe controlled	-0.212		
		SOM controlled	-0.240		
		Fe and SOM controlled	-0.112		
Zn	Spearman correlation coefficient		-0.338*	0.287*	0.319*
	Partial correlation coefficient	Fe controlled	-0.200		
		SOM controlled	-0.099		
		Fe and SOM controlled	-0.010		

* Correction is significant at the 0.01 level.

IV. DISCUSSION

A. VIS-NIR SPECTRAL INDEX PERFORMANCES IN ASSESSING SOIL HEAVY METALS

Many previous studies have investigated the potential of Vis-NIR spectra for the simultaneous estimation of the contents of various soil heavy metals [27], [38], [28], [46], [47]. In this study, we employed the PLSR model to define the Vis-NIR SIs using multivariate geostatistics to evaluate heavy metals in an agricultural area. The SIs contained the covariances of spectral variables and heavy metal variables. The optimal SIs for As, Pb and Zn, with the most covariance information, were obtained using PLSR based on the SG preprocessing method (Table 2), which could be because the SG method can effectively reduce the burr noise in the spectral measurement while preserving significant spectral information [48]. The unsatisfactory SIs based on the FD and SD spectra may be due to the enhancement of meaningful information and noise [49]. MSC and SNV can be used to reduce the estimation error caused by spectral baseline drift [26], and the unexceptional results for the SIs based on the SNC and MSC spectra may be due to the negligible change in the baseline.

An overlaying analysis of the kriged map indicated that the SIs defined in this paper were not sufficient to independently evaluate the spatial distribution of heavy metals, which may also be related to the low contents of the heavy metals. However, this issue will not be substantially discussed in this paper.

The performance indicators based on the cross-validation (Table 4) showed that the mapping of As and Zn using multivariate geostatistics with all covariables (Fe, SOM and SIs) was more unbiased and more accurate than the results heavy metals from the univariate geostatistics with only heavy metal datasets. This result indicated that Fe and SOM, as auxiliary information, can improve the prediction accuracy of soil heavy metals in low-content areas, which has also been

suggested in previous studies [28]. In particular, SIs were the most effective covariates compared with the SOM and Fe. It is also worth noting that Pb was insensitive to covariables. Considering the strong spatial autocorrelation and a few extreme values of Pb in the study area, we hypothesize that a sampling density of less than 2 km can fully express the spatial variability in Pb [50]. This may explain why the auxiliary variables did not improve the spatial prediction accuracy, although it is impossible to conclude that the SI of Pb is useless. Moreover, the correlation analysis between heavy metals and auxiliary variables is direct evidence that can be used to explain the performances of auxiliary variables in evaluating spatial distributions [6], [51]. All covariables were significantly correlated with heavy metals, and the higher significant associations (Table 5) also suggested that the SIs have the potential to be a substitute for soil properties, such as Fe and SOM, to improve the prediction accuracy of soil heavy metals.

B. EVALUATING THE SPECTRAL INDICES OF SOIL HEAVY METALS

Generally, an increase in heavy metal cations results in an increase in Fe oxides on the surfaces of clay and oxide minerals [25], [52]. Moreover, the decomposition of organic matter can greatly affect the enrichment of heavy metals in soil due to metal complexation [53], [54]. Spectrally featureless soil heavy metals can be estimated using the reflectance spectra of SOM and Fe oxides and clay [22], [52], [55]. Therefore, we infer that the SIs performed well because they contain comprehensive reflectance spectral information about soil properties such as SOM and Fe. Spearman correlation analysis and partial correlation analysis could be used to reveal the role of spectrally active soil properties (e.g., SOM and Fe) when evaluating the heavy metal content from reflectance spectra [27], [38]. Similarly, we use this strategy to explore

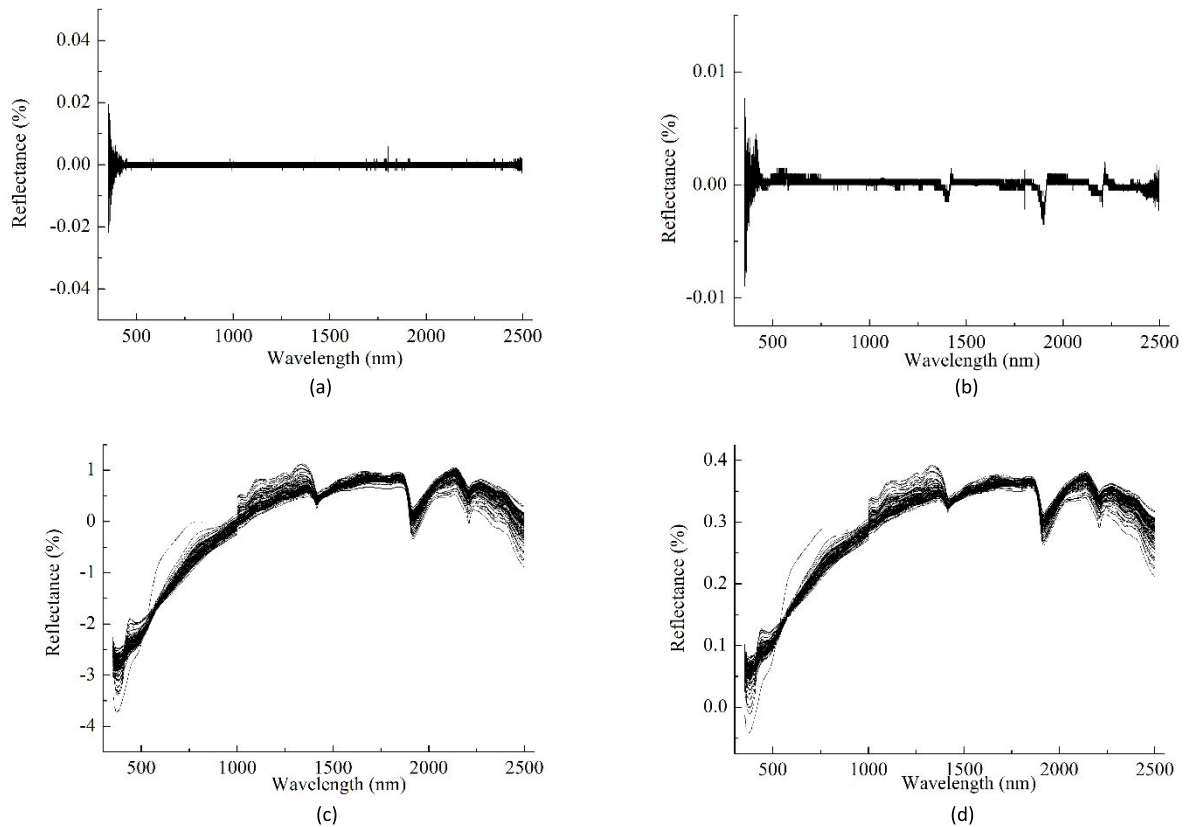


FIGURE 7. Preprocessed reflectance spectra of soil samples. (a) The 1st derivative spectra. (b) The 2nd derivative spectra. (c) SNV spectra. (d) MSC spectra.

TABLE 6. The covariance in the spectral indices of As, Pb and Zn with different SG parameters (%).

	Savitzky-Golay (order=0, framelen =3)		Savitzky-Golay (order=0, framelen =5)		Savitzky-Golay (order=0, framelen =7)		Savitzky-Golay (order=0, framelen =9)		Savitzky-Golay (order=0, framelen =11)	
	predictor	response	predictor	response	predictor	response	predictor	response	predictor	response
As	70	8	72	8	72	8	71	8	67	6
Pb	86	9	88	9	89	10	88	8	87	7
Zn	85	8	87	8	89	8	88	7	86	7

the mechanism of SIs. The results of the correlation and partial correlation analysis indicated that the contents of Fe and SOM were two important factors influencing SIs. Moreover, the important spectral analyses were to analyze the correlation of heavy metals with SOM and Fe from the perspective of spectral response. The VIP results (Fig. 3) showed that the important wavelengths of Fe, SOM and the three heavy metals mostly overlapped. This indicates that the SIs were closely related to Fe and SOM; in other words, the SIs contain spectral information that responds to Fe and SOM contents. Previous studies have demonstrated that the Vis-NIR can be used to indirectly evaluate soil heavy metals through the spectral responses of Fe and SOM [22], [27], [38], [46], [28] and [56]. Therefore, we confirm that the proposed SI is scientific and has the potential to be applied to other areas.

Based on the above discussion, we conclude that the auxiliary variable SIs contain comprehensive spectral information about soil properties (SOM and Fe) that can be used to characterize soil heavy metals. Due to limitations related to data collection, we only described the relationships of the SIs with SOM and Fe. In fact, the mineral particle size, soil parent material and other information can also be obtained from the reflectance spectrum [46].

V. CONCLUSION

In this study, a SI based on Vis-NIR spectroscopy was integrated with multivariate geostatistics to improve the mapping of soil heavy metals in an agricultural area of eastern China. The results indicated that the mean contents of As, Pb and Zn were slightly higher than the background values of the study area, and high values occurred at some sites. Through

SG spectral pretreatment, optimal SIs were obtained for As, Pb and Zn, which showed more covariance between spectra and heavy metal contents. The mapping approach based on SIs was unbiased and accurate compared with the OK predictors and OCK predictors using laboratory soil analyses (SOM and Fe). This demonstrated that our proposed SIs made a valuable contribution to the efficient prediction of heavy metals in low-concentration soils. Moreover, the SIs synthesized most information about soil properties (including SOM and Fe) that are used to characterize soil heavy metals. This result suggested that the proposed SI could be applied to other areas.

Future studies should continue to explore the proposed SI at different scales because the spectral response of soil heavy metals needs to take into account the intrinsic variations in soil properties.

APPENDIX

See Figure 7 and Table 6.

REFERENCES

- [1] B. J. Alloway, *Heavy Metals in Soils*. Dordrecht, The Netherlands: Springer, 2013.
- [2] J. A. Rodríguez Martín, C. De Arana, J. J. Ramos-Miras, C. Gil, and R. Boluda, "Impact of 70 years urban growth associated with heavy metal pollution," *Environ. Pollut.*, vol. 196, pp. 156–163, Jan. 2015.
- [3] J. A. Rodríguez Martín, J. J. Ramos-Miras, R. Boluda, and C. Gil, "Spatial relations of heavy metals in arable and greenhouse soils of a mediterranean environment region (Spain)," *Geoderma*, vols. 200–201, pp. 180–188, Jun. 2013.
- [4] H. Chen, Y. Teng, S. Lu, Y. Wang, and J. Wang, "Contamination features and health risk of soil heavy metals in china," *Sci. Total Environ.*, vols. 512–513, pp. 143–153, Apr. 2015.
- [5] Y. G. Gu, Q. S. Li, J. H. Fang, B. Y. He, H. B. Fu, and Z. J. Tong, "Identification of heavy metal sources in the reclaimed farmland soils of the pearl river estuary in China using a multivariate geostatistical approach," *Ecotoxicol. Environ. Saf.*, vol. 105, pp. 7–12, Jul. 2014.
- [6] Y.-Q. Song, A.-X. Zhu, X.-S. Cui, Y.-L. Liu, Y.-M. Hu, and B. Li, "Spatial variability of selected metals using auxiliary variables in agricultural soils," *Catena*, vol. 174, pp. 499–513, Mar. 2019.
- [7] S. Cao, A. Lu, J. Wang, and L. Huo, "Modeling and mapping of cadmium in soils based on qualitative and quantitative auxiliary variables in a cadmium contaminated area," *Sci. Total Environ.*, vol. 580, pp. 430–439, Feb. 2017.
- [8] Y. Liu, J. Lv, B. Zhang, and J. Bi, "Spatial multi-scale variability of soil nutrients in relation to environmental factors in a typical agricultural region, eastern china," *Sci. Total Environ.*, vols. 450–451, pp. 108–119, Apr. 2013.
- [9] Y. Jiang, S. Chao, J. Liu, Y. Yang, Y. Chen, A. Zhang, and H. Cao, "Source apportionment and health risk assessment of heavy metals in soil for a township in Jiangsu province, China," *Chemosphere*, vol. 168, pp. 1658–1668, Feb. 2017.
- [10] S.-W. Huang, J.-Y. Jin, L.-P. Yang, and Y.-L. Bai, "Spatial variability of soil nutrients and influencing factors in a vegetable production area of Hebei province in China," *Nutrient Cycling Agroecosystems*, vol. 75, nos. 1–3, pp. 201–212, Jul. 2006.
- [11] K. Phachomphon, P. Dlamini, and V. Chaplot, "Estimating carbon stocks at a regional level using soil information and easily accessible auxiliary variables," *Geoderma*, vol. 155, nos. 3–4, pp. 372–380, Mar. 2010.
- [12] Q.-Q. Li, T.-X. Yue, C.-Q. Wang, W.-J. Zhang, Y. Yu, B. Li, J. Yang, and G.-C. Bai, "Spatially distributed modeling of soil organic matter across china: An application of artificial neural network approach," *Catena*, vol. 104, pp. 210–218, May 2013.
- [13] P. Tziachris, V. Aschonitis, T. Chatzistathis, and M. Papadopoulou, "Assessment of spatial hybrid methods for predicting soil organic matter using DEM derivatives and soil parameters," *Catena*, vol. 174, pp. 206–216, Mar. 2019.
- [14] S. K. Behera, R. K. Mathur, A. K. Shukla, K. Suresh, and C. Prakash, "Spatial variability of soil properties and delineation of soil management zones of oil palm plantations grown in a hot and humid tropical region of southern India," *Catena*, vol. 165, pp. 251–259, Jun. 2018.
- [15] Y. Li, X. Fu, X. Liu, J. Shen, Q. Luo, R. Xiao, Y. Li, C. Tong, and J. Wu, "Spatial variability and distribution of N₂O emissions from a tea field during the dry season in subtropical central China," *Geoderma*, vols. 193–194, pp. 1–12, Feb. 2013.
- [16] S. Salvador-Blanes, S. Cornu, A. Couturier, D. King, and J.-J. Macaire, "Morphological and geochemical properties of soil accumulated in hedge-induced terraces in the Massif Central, France," *Soil Tillage Res.*, vol. 85, nos. 1–2, pp. 62–77, Jan. 2006.
- [17] R. Bou Kheir, B. Shomar, M. B. Greve, and M. H. Greve, "On the quantitative relationships between environmental parameters and heavy metals pollution in Mediterranean soils using GIS regression-trees: The case study of Lebanon," *J. Geochem. Explor.*, vol. 147, pp. 250–259, Dec. 2014.
- [18] S. Maas, R. Scheifler, M. Benslama, N. Crini, E. Lucot, Z. Brahmia, S. Benyacoub, and P. Giraudoux, "Spatial distribution of heavy metal concentrations in urban, suburban and agricultural soils in a Mediterranean city of Algeria," *Environ. Pollut.*, vol. 158, no. 6, pp. 2294–2301, Jun. 2010.
- [19] D. Sollitto, M. Romic, A. Castrignanò, D. Romic, and H. Bakic, "Assessing heavy metal contamination in soils of the Zagreb region (Northwest Croatia) using multivariate geostatistics," *Catena*, vol. 80, no. 3, pp. 182–194, Mar. 2010.
- [20] J. A. Rodríguez, N. Nanos, J. M. Grau, L. Gil, and M. López-Arias, "Multiscale analysis of heavy metal contents in Spanish agricultural topsoils," *Chemosphere*, vol. 70, no. 6, pp. 1085–1096, Jan. 2008.
- [21] J. Lv, Y. Liu, Z. Zhang, and B. Dai, "Multivariate geostatistical analyses of heavy metals in soils: Spatial multi-scale variations in Wulian, Eastern China," *Ecotoxicol. Environ. Saf.*, vol. 107, pp. 140–147, Sep. 2014.
- [22] Y. Wu, J. Chen, J. Ji, P. Gong, Q. Liao, Q. Tian, and H. Ma, "A mechanism study of reflectance spectroscopy for investigating heavy metals in soils," *Soil Sci. Soc. Amer. J.*, vol. 71, no. 3, pp. 918–926, May 2007.
- [23] T. Kemper and S. Sommer, "Use of airborne hyperspectral data to estimate residual heavy metal contamination and acidification potential in the Guadiamar floodplain Andalusia, Spain after the Aznalcollar mining accident," *Proc. SPIE*, vol. 5574, pp. 224–234, Oct. 2004.
- [24] E. Choe, F. van der Meer, F. van Ruitenbeek, H. van der Werff, B. de Smeth, and K.-W. Kim, "Mapping of heavy metal pollution in stream sediments using combined geochemistry, field spectroscopy, and hyperspectral remote sensing: A case study of the Rodalquilar mining area, SE Spain," *Remote Sens. Environ.*, vol. 112, no. 7, pp. 3222–3233, Jul. 2008.
- [25] T. Shi, L. Guo, Y. Chen, W. Wang, Z. Shi, Q. Li, and G. Wu, "Proximal and remote sensing techniques for mapping of soil contamination with heavy metals," *Appl. Spectrosc. Rev.*, vol. 53, no. 10, pp. 783–805, Mar. 2018.
- [26] T. Shi, H. Liu, Y. Chen, T. Fei, J. Wang, and G. Wu, "Spectroscopic diagnosis of arsenic contamination in agricultural soils," *Sensors*, vol. 17, no. 5, p. 1036, May 2017.
- [27] M. St. Luce, N. Ziadi, B. Gagnon, and A. Karam, "Visible near infrared reflectance spectroscopy prediction of soil heavy metal concentrations in paper mill biosolid- and liming by-product-amended agricultural soils," *Geoderma*, vol. 288, pp. 23–36, Feb. 2017.
- [28] J. Wang, L. Cui, W. Gao, T. Shi, Y. Chen, and Y. Gao, "Prediction of low heavy metal concentrations in agricultural soils using visible and near-infrared reflectance spectroscopy," *Geoderma*, vol. 216, pp. 1–9, Mar. 2014.
- [29] M. Zovko, D. Romić, C. Colombo, E. Di Iorio, M. Romić, G. Buttafuoco, and A. Castrignanò, "A geostatistical vis-NIR spectroscopy index to assess the incipient soil salinization in the Neretva River valley, Croatia," *Geoderma*, vol. 332, pp. 60–72, Dec. 2018.
- [30] J. G. Cobo, G. Dercon, T. Yekeye, L. Chapungu, C. Kadzere, A. Murwira, R. Delve, and G. Cadisch, "Integration of mid-infrared spectroscopy and geostatistics in the assessment of soil spatial variability at landscape level," *Geoderma*, vol. 158, nos. 3–4, pp. 398–411, Sep. 2010.
- [31] S. S. Paul, N. C. Coops, M. S. Johnson, M. Krzic, and S. M. Smukler, "Evaluating sampling efforts of standard laboratory analysis and mid-infrared spectroscopy for cost effective digital soil mapping at field scale," *Geoderma*, vol. 356, Dec. 2019, Art. no. 113925.
- [32] T. Chen, Q. Chang, J. Liu, J. G. P. W. Clevers, and L. Kooistra, "Identification of soil heavy metal sources and improvement in spatial mapping based on soil spectral information: A case study in northwest China," *Sci. Total Environ.*, vol. 565, pp. 155–164, Sep. 2016.

- [33] C.-F. Li, F. Wang, W.-T. Cao, J. Pan, J.-S. Lv, and Q.-Y. Wu, "Source analysis, spatial distribution and pollution assessment of heavy metals in sewage irrigation area farmland soils of Longkou City," *Environ. Sci.*, vol. 38, no. 3, pp. 1018–1027, Mar. 2017.
- [34] Y. Shan and L. Wu, "Analysis of water resources supply and demand in Longkou City," (in Chinese), *Shandong Water Resource.*, no. 4, pp. 36–37, May 2013.
- [35] J. Lv, Y. Liu, Z. Zhang, and J. Dai, "Factorial kriging and stepwise regression approach to identify environmental factors influencing spatial multi-scale variability of heavy metals in soils," *J. Hazardous Mater.*, vol. 261, pp. 387–397, Oct. 2013.
- [36] Y. Liu and Y. Chen, "Estimation of total iron content in floodplain soils using VNIR spectroscopy—A case study in the Le'an River floodplain, China," *Int. J. Remote Sens.*, vol. 33, no. 18, pp. 5954–5972, May 2012.
- [37] Y. Liu, Q. Jiang, T. Fei, J. Wang, T. Shi, K. Guo, X. Li, and Y. Chen, "Transferability of a visible and near-infrared model for soil organic matter estimation in riparian landscapes," *Remote Sens.*, vol. 6, no. 5, pp. 4305–4322, May 2014.
- [38] H. Cheng, R. Shen, Y. Chen, Q. Wan, T. Shi, J. Wang, Y. Wan, Y. Hong, and X. Li, "Estimating heavy metal concentrations in suburban soils with reflectance spectroscopy," *Geoderma*, vol. 336, pp. 59–67, Feb. 2019.
- [39] Y. Hong, L. Yu, Y. Chen, Y. Liu, Y. Liu, Y. Liu, and H. Cheng, "Prediction of soil organic matter by VIS-NIR spectroscopy using normalized soil moisture index as a proxy of soil moisture," *Remote Sens.*, vol. 10, no. 2, p. 28, Dec. 2017.
- [40] C. Gomez, P. Lagacherie, and G. Coulouma, "Continuum removal versus PLSR method for clay and calcium carbonate content estimation from laboratory and airborne hyperspectral measurements," *Geoderma*, vol. 148, no. 2, pp. 141–148, Dec. 2008.
- [41] D. Y. Kenett, X. Huang, I. Vodenska, S. Havlin, and H. E. Stanley, "Partial correlation analysis: Applications for financial markets," *Quant. Finance*, vol. 15, no. 4, pp. 569–578, Mar. 2015.
- [42] B. Schaffrin, "Minimum mean squared error (MSE) adjustment and the optimal Tykhonov-Phillips regularization parameter via reproducing best invariant quadratic uniformly unbiased estimates (repro-BIQUEE)," *J. Geodesy*, vol. 82, no. 2, pp. 113–121, Sep. 2007.
- [43] S. S. Carroll and N. Cressie, "A comparison of geostatistical methodologies used to estimate snow water equivalent," *J. Amer. Water Resour. Assoc.*, vol. 32, pp. 267–278, Jun. 2007.
- [44] *State Environmental Protection Administration of China, Environmental Quality Standard for Soils*, Standard GB15618-1995, Standards Press of China, Beijing, China, 1997.
- [45] *China National Environmental Monitoring Center, Background contents of Elements in Soils of China*, China Environ. Sci. Press, Beijing, China, 1990.
- [46] T. Shi, Y. Chen, Y. Liu, and G. Wu, "Visible and near-infrared reflectance spectroscopy—An alternative for monitoring soil contamination by heavy metals," *J. Hazardous Mater.*, vol. 265, pp. 166–176, Jan. 2014.
- [47] J. Liu, Y. Zhang, H. Wang, and Y. Du, "Study on the prediction of soil heavy metal elements content based on visible near-infrared spectroscopy," *Spectrochim. Acta A, Mol. Biomolecular Spectrosc.*, vol. 199, pp. 43–49, Jun. 2018.
- [48] W. Sun, X. Zhang, B. Zou, and T. Wu, "Exploring the potential of spectral classification in estimation of soil contaminant elements," *Remote Sens.*, vol. 9, no. 6, p. 632, Jun. 2017.
- [49] T. Chen, Q. Chang, J. G. P. W. Clevers, and L. Kooistra, "Rapid identification of soil cadmium pollution risk at regional scale based on visible and near-infrared spectroscopy," *Environ. Pollut.*, vol. 206, pp. 217–226, Nov. 2015.
- [50] T. Chen, X. Liu, X. Li, K. Zhao, J. Zhang, J. Xu, J. Shi, and R. A. Dahlgren, "Heavy metal sources identification and sampling uncertainty analysis in a field-scale vegetable soil of hangzhou, china," *Environ. Pollut.*, vol. 157, no. 3, pp. 1003–1010, Mar. 2009.
- [51] X. Fei, G. Christakos, R. Xiao, Z. Ren, Y. Liu, and X. Lv, "Improved heavy metal mapping and pollution source apportionment in Shanghai City soils using auxiliary information," *Sci. Total Environ.*, vol. 661, pp. 168–177, Apr. 2019.
- [52] P. Rathod, D. G. Rossiter, M. F. Noomen, and F. D. van der Meer, "Proximal spectral sensing to monitor phytoremediation of metal-contaminated soils," *Int. J. Phytoremediation*, vol. 15, no. 5, pp. 405–426, May 2013.
- [53] A. Piccolo and F. J. Stevenson, "Infrared spectra of Cu^{2+} Pb^{2+} and Ca^{2+} complexes of soil humic substances," *Geoderma*, vol. 27, no. 3, pp. 195–208, Apr. 1982.
- [54] M. Egli, P. Fitze, and M. Oswald, "Changes in heavy metal contents in an acidic forest soil affected by depletion of soil organic matter within the time span 1969–93," *Environ. Pollut.*, vol. 105, no. 3, pp. 367–379, Jun. 1999.
- [55] D. F. Malley and P. C. Williams, "Use of near-infrared reflectance spectroscopy in prediction of heavy metals in freshwater sediment by their association with organic matter," *Environ. Sci. Technol.*, vol. 31, pp. 3461–3467, Jun. 1997.
- [56] Y. Hong, R. Shen, H. Cheng, Y. Chen, Y. Zhang, Y. Liu, M. Zhou, L. Yu, Y. Liu, and Y. Liu, "Estimating lead and zinc concentrations in peri-urban agricultural soils through reflectance spectroscopy: Effects of fractional-order derivative and random forest," *Sci. Total Environ.*, vol. 651, pp. 1969–1982, Feb. 2019.



JIANFEI CAO was born in Linyi, China, in 1991. He received the M.Sc. degree from Shandong Normal University, China, in 2019, where he is currently pursuing the Ph.D. degree in cartography and geographic information systems with the College of Geography and Environment.

Since September 2019, he has been a Geographic Information and Mapping Engineer. His main research interests are in soil remote sensing monitoring, soil mapping research, and GIS software development.



CHUNFANG LI was born in 1989. She received the Ph.D. degree from Shandong Normal University, China, in 2019. She is currently a Lecturer with Shandong Jiaotong University, China. Her main research interests are in spatial-temporal data crawling, environmental remote sensing, hyperspectral remote sensing, and remote sensing image retrieval.



QUANYUAN WU was born in 1959. He received the Ph.D. degree from the Shandong University of Science and Technology, Qingdao, China, in 2007.

Since 2003, he has been a Professor with the Department of Geography, College of Geography and Environment, Shandong Normal University. His research interests include the development of remote sensing and geographic information techniques.

Dr. Wu is a member of the Education and Science Popularization Committee of the China GIS Association, the Executive Director of the Shandong Remote Sensing Society, the Executive Director of the Shandong Land Society, and the Winner of the First Shandong Youth Science and Technology Award. He presided over or participated in three national natural science foundations of China.



JIANMIN QIAO was born in 1988. He received the Ph.D. degree from Beijing Normal University, Beijing, China, in 2018.

In September 2018, he became a Lecturer with the College of Geography and Environment, Shandong Normal University. His research interests include agricultural ecosystem service and landscape sustainability.